Effect of cooling rate on the interlaminar fracture toughness of unidirectional Carbon/PPS laminates

Francisco Sacchetti[1,2], Wouter J.B. Grouve[1], Laurent L. Warnet[2], Irene Fernandez Villegas[3]

[1]*ThermoPlastic composites Research Center (TPRC), Enschede, The Netherlands*

[2]*Faculty of Engineering Technology, Chair of Production Technology, University of Twente, Enschede, The Netherlands*

[3]*Structural Integrity and Composites, Faculty of Aerospace Engineering, Delft University of Technology, Delft, The Netherlands*

Palatijn 15, P.O. Box 770, 7500AE Enschede, The Netherlands

Email: Laurent Warnet (l.warnet@ utwente.nl), web page: http://www.tprc.nl

Effect of cooling rate on the interlaminar fracture toughness of unidirectional Carbon/PPS laminates

Abstract

The effect of cooling rate on the interlaminar fracture toughness of Carbon reinforced PPS laminates was investigated experimentally. A typical stamp forming process was utilised in a *novel manner to achieve high average cooling rates, of up to 3500 °C/minute, while ensuring a good consolidation* quality. Differential scanning calorimetry measurements were used to characterise the degree of crystallinity of the samples, while the interlaminar fracture toughness of the laminates was characterised under mode I using the Double Cantilever Beam test. Finally, micrographic analysis of the fracture surfaces was carried out to correlate the degree of crystallinity to the failure modes. A strong correlation between fracture toughness and degree of crystallinity was found. The samples with a low degree of crystallinity showed a high interlaminar fracture toughness and large plastic deformation of the matrix during fracture.

1 Introduction

Thermoplastic composites are of increasing interest to the aerospace and automotive industries. Compared to many metals, they provide a higher specific strength and stiffness, an increased design freedom and the ability to tailor mechanical performance to the particular application [1]. Moreover, the melt-processability of the thermoplastic matrix allows high production rates, assembly through fusion bonding and makes recycling easier as the matrix and fibres do not necessarily need to be separated [2, 3]. Arguably, the main bottleneck preventing broader application of thermoplastic composites is the final part costs. To overcome this, efforts have been made to cut manufacturing costs through automation and by reducing cycle times. This has resulted in the industrialisation of new manufacturing technologies such as stamp forming [4-6], which in some cases is found to be more cost efficient than the previously existing thermoset manufacturing processes. Moreover, new promising thermoplastic composite production techniques such as laser assisted fibre placement, over-injection moulding, pultrusion, and ultrasonic welding are under continuous development, with the aim of further reducing the manufacturing costs. All of these new processing techniques are characterised by having high cooling rates, ranging from 400 °C/min for pultrusion [7] up to 24000 °C/min for automated fibre placement (AFP) [8]. Changes pertaining to the large cooling rates during manufacturing are known to affect the mechanical performance of the final thermoplastic composite parts. Therefore, the interest in the effect of fast cooling rates on the mechanical performance of thermoplastic composites is becoming more relevant with the advancement of these new technologies. Unfortunately, process optimisation of the new manufacturing technologies is challenging as the characteristic processing conditions, cooling rate in particular, still lie outside the known process-property envelope. This makes it difficult to predict the mechanical performance of the final part. Clearly, there is a need to extend the known process-property envelope for a

range of materials in order to fully utilise the potential of thermoplastic composites.

The effect of processing conditions, and in particular cooling rate, on the mechanical properties of Carbon fibre reinforced Polyphenylene-sulphide (Carbon/PPS) [9-13] and Carbon fibre reinforced Polyether-ether-ketone (Carbon/PEEK) composites [14-25], has received extensive attention in the literature. A common finding is that properties such as the fibre-matrix interfacial shear strength (IFSS) [19, 22], tensile strength [12, 13], tensile modulus [12, 18] and interlaminar shear strength [10, 11] decrease with increasing cooling rate. However, matrix ductility and interlaminar fracture toughness increase with increasing cooling rate [20-25]. These changes in mechanical performance have been mainly correlated to a change in the degree of crystallinity of the polymeric matrix.

Among the studies mentioned in the previous paragraph, the ones focusing on continuous fibre composites utilised autoclave or hot press consolidation as manufacturing techniques, achieving maximum cooling rates of around 80°C/min. Efforts were made by some research groups to obtain higher cooling rates. However, cooling rates above 100 °C/min and up to 2000°C/min could only be achieved by releasing the consolidation pressure in order to bring the material in contact with a heat sink (either water or aluminium plates) [24, 25]. The releasing of pressure affected the quality of the laminates, evidenced by the presence of voids [24]. Consequently, interpreting the results obtained from mechanical testing of these specimens was problematic since they were influenced by both the presence of voids and the change in crystallinity.

The present work focuses on extending knowledge about the influence of high cooling rates on interlaminar fracture toughness of Carbon/PPS laminates. The interlaminar fracture toughness is of interest as it is sensitive to the polymer properties and thus the processing conditions. As an alternative approach, the present work proposes using a stamp forming process to manufacture well consolidated specimens with a high cooling rate. A stamp

forming process was used where the tool temperature controls the cooling rate. Three mould temperatures were used, namely 200 °C, 100 °C and 25 °C. After manufacturing, the degree of crystallinity of the specimens was measured using Differential Scanning Calorimetry (DSC). The effect of the degree of crystallinity on the interlaminar fracture toughness was investigated using Double Cantilever Beam (DCB) testing. Finally, the fracture surfaces of the samples were analysed to correlate the degree of crystallinity with the failure modes.

2 Experimental methods

This section describes the materials used in this research, followed by the description of the processes used to manufacture the samples. After processing, DSC measurements, mode I interlaminar fracture toughness tests and SEM fractographic analysis were used to characterise the samples. The methodology followed to perform the measurments is described in this section.

2.1 Materials & laminate consolidation

Unidirectional Carbon Polyphenylene-sulphide (Carbon/PPS) pre-preg material (Cetex TC1100 produced by TenCate Advanced Composites) was used in this research. The PPS matrix used in the pre-preg is a semicrystalline polymer with glass transition and melting temperature of 90 °C and 280 °C, respectively. The composite material has a matrix content of 34 % by weight. Flat laminates, with a stacking sequence of $[0]_{12}$, were press consolidated in a Pinette hot platen press to be used as blanks in a subsequent stamp forming step. A picture frame mould, with a cavity dimension of 300 by 300 mm^2, was used to avoid excessive flow of the material during consolidation. The press consolidation cycle suggested by TenCate was used to manufacture the laminates and is shown in Figure 3.1. It can be seen that a nominal cooling rate of 5 °C/min was used. Three types of laminates were manufactured and are schematically illustrated in Figure 3.2:

Type I: The first type was used for temperature measurements. One type K thermocouple was located at the laminate's midplane to measure the temperature during stamp forming, thereby evaluating the cooling rate.

Type II: The second type was used for mechanical testing. A 13 µm thick polyimide film was inserted at one of the edges of the laminate at the midplane in order to provide the pre-crack required for DCB testing.

Type III: The last type was used for DSC measurements. This laminate featured a polyimide film between each ply for the first six plies. The polyimide films allow separation of the plies after manufacturing. In this way, the degree of crystallinity through the thickness of the laminate can be evaluated. Only one laminate of this type was prepared.

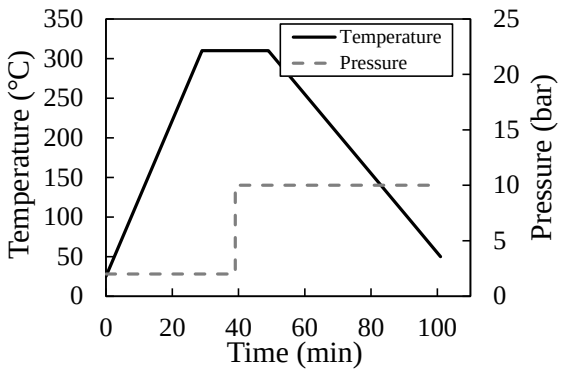

Figure 1: Press consolidation cycle for the Carbon/PPS laminates

One additional type II laminate was prepared but not stamp formed. Instead, it was kept as reference for the press consolidation process. The nominal laminate thickness after press consolidation was 1.8 mm. This low thickness was intended to enable high cooling rates during the subsequent stamp forming process and, more or less, a uniform temperature distribution through the thickness of the laminate.

2.2 Stamp forming process

The Pinette hot platen press was also used for stamp forming the pre-consolidated laminates. The stamp forming setup consists of an infrared oven and a transport system to automatically

transfer the blanks from a loading station to the oven, and from the oven to the forming station. During stamp forming, the laminates were pre-heated in the infrared oven with an area of 700 by 8000 mm^2 to reach a temperature of 320 °C as measured with a thermocouple. Subsequently, they were transferred to the press station and stamp formed between two flat aluminium moulds measuring 250 by 250 mm^2 at a pressure of 20 bar for 1 minute. As the infrared oven is more than 2 times bigger than the laminates, uniform in plane temperature was assumed. The cooling rate of the laminates from a temperature of 320 °C to the mould temperature was dictated by the mould temperature. Three mould temperatures, equal for both mould halves, were used: 200 °C, 100 °C and 25 °C. It is worth noticing that the typical mould temperature for stamp forming of Carbon/PPS parts is 200 °C. A LabVIEW data acquisition system was used to record the temperature from the

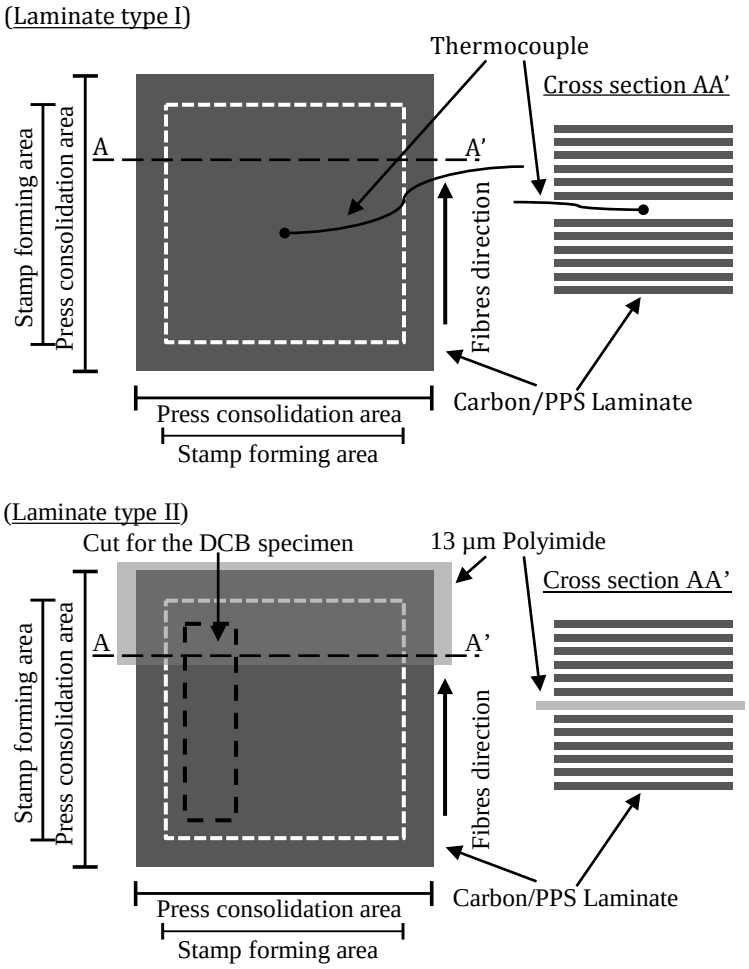

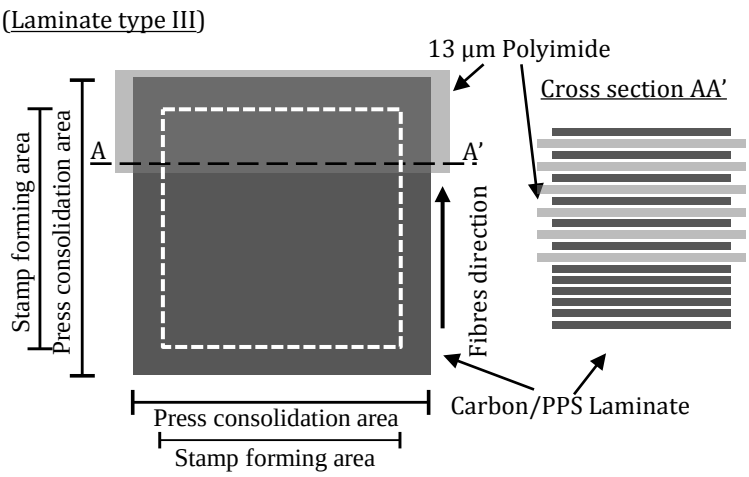

Figure 2: Schematic view of the lay-up of the three types of laminates produced in this study.

thermocouple embedded in the type I laminates during the stamp forming process. After the stamp forming cycle, the laminates were allowed to further cool down from mould temperature to room temperature by natural convection. The time required for heating up was measured using the laminates of type I. For the laminates of type II and type III only the heating time was used, and not the actual temperature measured on them.

Two laminates were manufactured for each stamping mould temperature. One laminate was used to measure the temperature (laminate type I), while the other one was used for physical and mechanical testing (laminate type II). An additional laminate with polyimide films in between the first six plies (laminate type III) was stamp formed using a mould temperature of 25°C. Cross-sectional micrographs were obtained from all type II laminates with a Leica DMRX optical microscope. The micrographs were used to assess the presence of voids after stamp forming.

After measuring the interlaminar fracture toughness in the type II laminates stamp formed at 100 °C and 25 °C mould temperature, the already tested specimens were subjected to an annealing treatment in order to increase their crystallinity fraction. This treatment was aimed at obtaining the same level of crystallinity as obtained in the press-consolidated samples. The annealing treatment involved placement of the specimens in a pre-heated convection oven at

180 °C for 30 minutes without the application of pressure [26]. After the annealing treatment, the degree of crystallinity and the interlaminar fracture toughness of the specimens were measured again.

Sample name	Consolidation technique	Laminates type
Reference	Press consolidated	II
S-200	Stamp formed with moulds at 200°C	I,II
S-100	Stamp formed with moulds at 100°C	I,II
S-25	Stamp formed with moulds at 25°C	I,II,II
S-100-a	Stamp formed with moulds at 100°C- annealed	II
S-25-a	Stamp formed with moulds at 25°C-annealed	II

Table 3.1: Summary of the sample names, the production technology used and the type of laminates produced for each condition.

Table 3.1 summarises all prepared samples, with their designated name, the processing technology used to manufacture the sample, and the type of laminates that were prepared. The laminate that was only subjected to press consolidation is listed as Reference sample. The name of the samples that were stamp formed start with an S followed by number which indicates the temperature of the moulds during the stamp forming process (that is S-200, S-100 and S-25 for samples that were stamp formed using moulds at 200, 100 and 25 °C, respectively). In the case of samples that were subjected to an annealing treatment, an “a” was added at the end of the name (S-100-a and S-25-a).

2.3 Differential Scanning Calorimetry experiments

The degree of crystallinity of each laminate type II and type III was measured by differential scanning calorimetry. A Mettler Toledo differential scanning calorimeter (DSC822E) was used for this purpose. The measurements were performed in a Nitrogen atmosphere with heating and cooling rates of 10 °C/min from room temperature to 320 °C and vice versa. A drop of silicon paste was added between the specimen and the crucible to improve thermal contact and to hence increase the accuracy of the first heating run. For the DSC analysis, at least three specimens of at least 10 mg were taken from the central part of each laminate. Since all the laminates used in this study had a thickness of around 1.8 mm, it was assumed,

following previous works [27], that the degree of crystallinity did not vary much over the thickness of the specimen. As mentioned earlier, this assumption was cross-checked by performing DSC measurements on the individual plies from a laminate with polyimide films between the first six plies, for the laminate processed with the highest cooling rate (laminate S-25 type III).

The degree of crystallinity was calculated by analysing only the heating run using the following equation [13]:

$$X_c = \frac{\Delta H_f + \Delta H_c}{(1 - W_f)\Delta H_f^0}, \tag{1}$$

where, W_f is the weight fraction of reinforcing fibre in the composite (66 % for the material used in this research), ΔH_f is the enthalpy of fusion, ΔH_c is the enthalpy of cold crystallization, and ΔH_f^0 is the fusion enthalpy of 100 % crystalline PPS. Values of ΔH_f^0 found in the literature for PPS range from about 50 J/g to 150.4 J/g [13]. The latter was used in this study to calculate the degree of crystallinity, as that value was measured for TenCate material.

2.4 Double cantilever beam experiments

The interlaminar fracture toughness of the different samples was characterised using double cantilever beam testing. Four specimens were cut per sample in the longitudinal direction of the fibres and then tested according to ISO 15024. The specimens were cut such that they had an initial crack length of about 55±10 mm. The specimens were loaded in a servohydraulic Instron 8500 universal testing machine equipped with a 200 N force cell. Before testing, a mode I pre-crack was created according to the procedure indicated in the ISO 15024 standard. Both pre-cracking and the DCB tests were performed at a crosshead speed of 4.8 mm/min.

The energy release rate (G_{IC}) was calculated using the corrected beam theory (CBT) data

reduction method as:

$$G_{IC} = \frac{3P\delta}{2w(x+\Delta)}\frac{1}{N}, \tag{2}$$

with w the specimen width, P and delta the applied force and displacement, respectively, and x the crack tip location as defined in Figure 3. The latter was measured during the test using an automated travelling camera system. Two correction factors N and Δ were used. The former accounts for the stiffening effects of the loading blocks, while the latter accounts for root rotation at the crack tip. There is no need for a large deformation correction factor, designated as F in the standard, as the travelling camera system was used to measure x, as opposed to the crack length a [28].

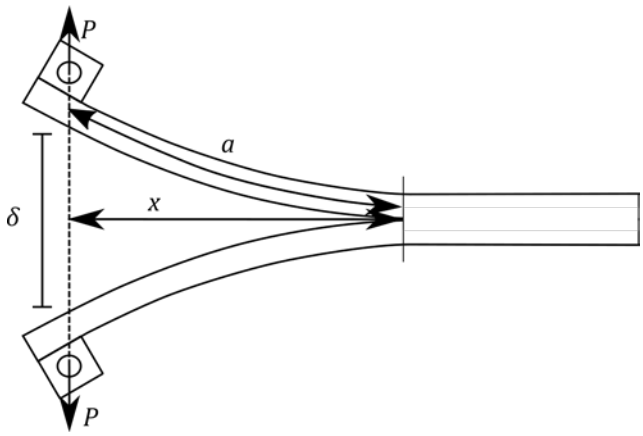

Figure 3 Schematic illustration of a DCB specimen undergoing large displacement. Image reproduced from Williams [28].

The interlaminar fracture toughness was calculated for both crack initiation and crack propagation. The maximum force criteria was used to evaluate the initiation point, from that point onwards the G_{IC} values were considered as propagation values. An example of force vs. displacement curve for the pre-crack and for the DCB test of a press-consolidated specimen is shown in Figure 3.4.

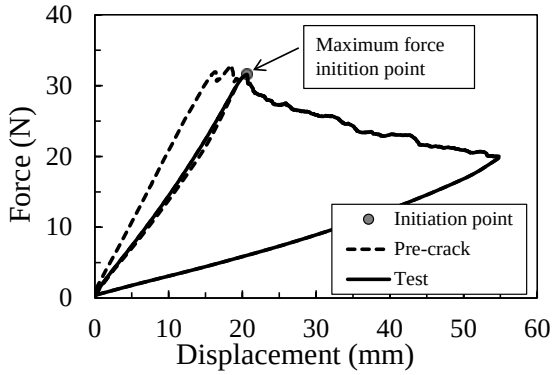

Figure 4: Example of a force vs. displacement curve during pre-cracking and testing of a DCB specimen.

As mentioned earlier, the specimens from samples S-100 and S-25 were subjected to an annealing treatment after testing. Before (re-)testing the annealed specimens, they were cut to have an initial crack length of 55±10 mm. No pre-cracking was needed as these specimens already had a pre-crack from the previous test.

3 Experimental results

The current section presents the experimental results. Firstly, the cooling rates as measured during the stamp forming process are presented, followed by cross-sectional micrographs after stamp forming. Secondly, the results of differential scanning calorimetry and the interlaminar fracture toughness measurements are provided and discussed. Finally, the fractographic analysis is presented, where the observed failure modes are correlated to the degree of crystallinity.

3.1 Cooling rates during stamp forming

The objective of using the stamp forming process in this study was to achieve cooling rates that limit the PPS crystallisation process while keeping sufficient consolidation pressure. Figure 3.5 shows the temperature at the midplane of the laminate versus time for the stamp forming process with the three mould temperatures. The temperature traces were recorded during the stamp forming of type I laminates. The graph on the right in Figure 3.5 shows a

detailed view of the cooling phase. As expected, the cooling rate decreases with increasing mould temperature. For each mould temperature, the cooling rate was calculated at four different temperatures. These were the temperature at the beginning of the stamp forming stage (320 °C), at the reported melting temperature of PPS (T_m = 280 °C), at the temperature at which the crystallisation rate of PPS is the highest and is approximated to ([(T_m-T_g)/2] = 185 °C), and at the reported glass transition temperature T_g of PPS (90 °C). It is worth noticing that the cooling rate cannot be directly correlated to the final degree of crystallinity as isothermal crystallisation occurs above T_g [26]. The cooling rates as a function of mould temperature are shown in Table 3.2. It can be noted that the cooling rates achieved are significantly higher than the ones usually observed during traditional consolidation techniques, typically 5 °C/min for press consolidation.

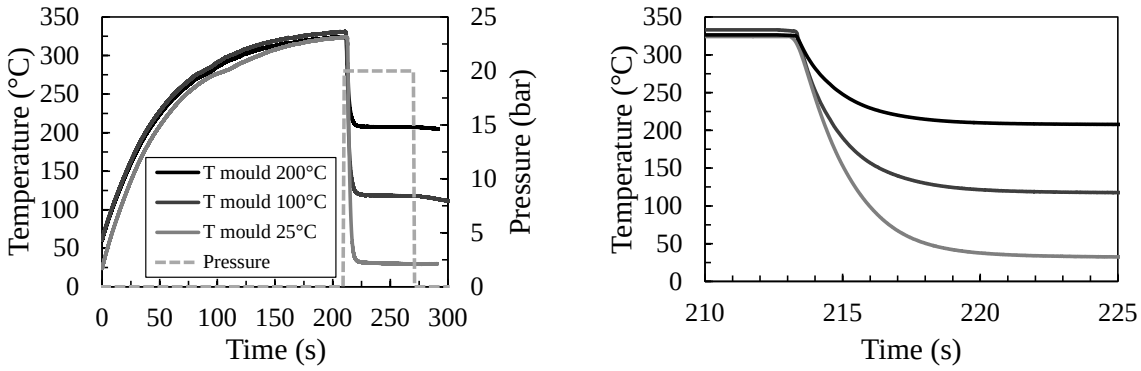

Figure 5: Left: Midplane laminate temperature vs. time curves for the different mould temperatures as observed during the stamp forming process. Right: a detailed look at the cooling phase.

Mould temperature:	Cooling rate at 320 °C	Cooling rate at 280 °C (T_m)	Cooling rate at 185 °C [(T_m-T_g)/2]	Cooling rate at 90 °C (T_g)
200 °C	4200 °C/min	3300 °C/min	-	-
100 °C	7600°C/min	6500 °C/min	2400 °C/min	-
25 °C	7400°C/min	6500 °C/min	4800 °C/min	2200 °C/min

Table 3.2: Cooling rates measured in the stamp consolidation process.

The stamp-formed type II laminates were checked for voids by inspecting cross-sectional micrographs. No voids were observed in any of the cross sections. Hence, consolidation was

assumed to be satisfactory for all specimens. Differences in the transparency of the matrix in different samples could be observed by using dark field microscopy. Figure 3.6 shows examples of the cross-sectional micrographs. Although difficult to see from the printed micrographs, the dark field microscopy showed differences in matrix appearance. The matrix in the Reference and S-200 sample had a whitish colour, while the matrix material S-25 sample was transparent. This is a first indication of differences in degree of crystallinity.

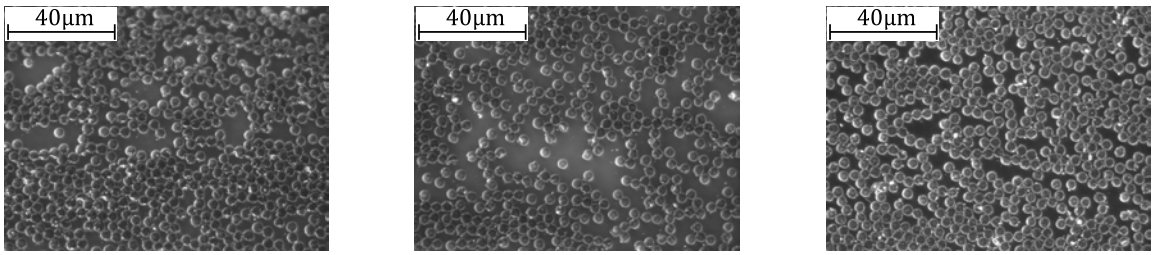

Figure 6: Cross-sectional micrographs. From left to right: Reference sample, stamp-formed sample with moulds at 200°C (S-200), and a stamp-formed sample with moulds at 25°C (S-25).

3.2 Differential scanning calorimetry measurements (DSC)

Table 3.3 shows the average degree of crystallinity of the first six plies of the S-25 laminate (laminate type III). It can be observed that the variability in the degree of crystallinity over the thickness of the laminate is small and that it lies close to the scatter of the testing technique. These results validate the simplified approach of using a bulk measurement to represent the degree of crystallinity at the midplane of the laminates used in the rest of this study.

Figure 3.7 shows the DSC heating curves for a few specimens. The trace of a S-100-a specimen is not shown in the Figure as it is similar to the trace of a S-25-a specimen. The S-100 and S-25 specimens showed an exothermic cold crystallisation peak in the temperature range from 100°C to 140°C. This peak was not found in the other curves. The second clear peak observed is an endothermic peak which was observed in all the specimens lying in the range from 250 °C to 290 °C and corresponds to the melting of the crystalline phase. Finally,

the S-200 and S-25-a specimens showed an additional small peak in the vicinity of 220 °C for the S-200 specimen and 190 °C for the S-25-a specimen. The bottom left graph in Figure 3.7 shows these peaks in closer detail. A similar small peak in the vicinity of 190 °C was also observed for the S-100-a specimen. These small peaks can be associated with the melting of a small fraction of a secondary population of lamella formed when crystallisation occurs at a temperature below 280 °C [29, 30]. Such secondary fusion peaks are known to appear at a temperature just above the temperature at which the secondary crystallisation occurred [29, 30]. It means close to 180°C for both annealed specimens (S-100-a and S-25-a) and close to 200 °C for the S-200 specimen.

Sample	Degree of crystallinity (%)
S-25-1st ply	9.8±1.0
S-25-2nd ply	11.6±1.2
S-25-3rd ply	13.6±1.4
S-25-4th ply	13.7±2.1
S-25-5th ply	12.1±1.5
S-25-6th ply	11.9±1.8

Table 3.3: Through thickness crystallinity for the S-25 sample, with the 1st ply being the outermost ply of the laminate and the 6th ply at the centre of the laminate. The reported values correspond to the average and the standard deviation of three measurements for each separate ply.

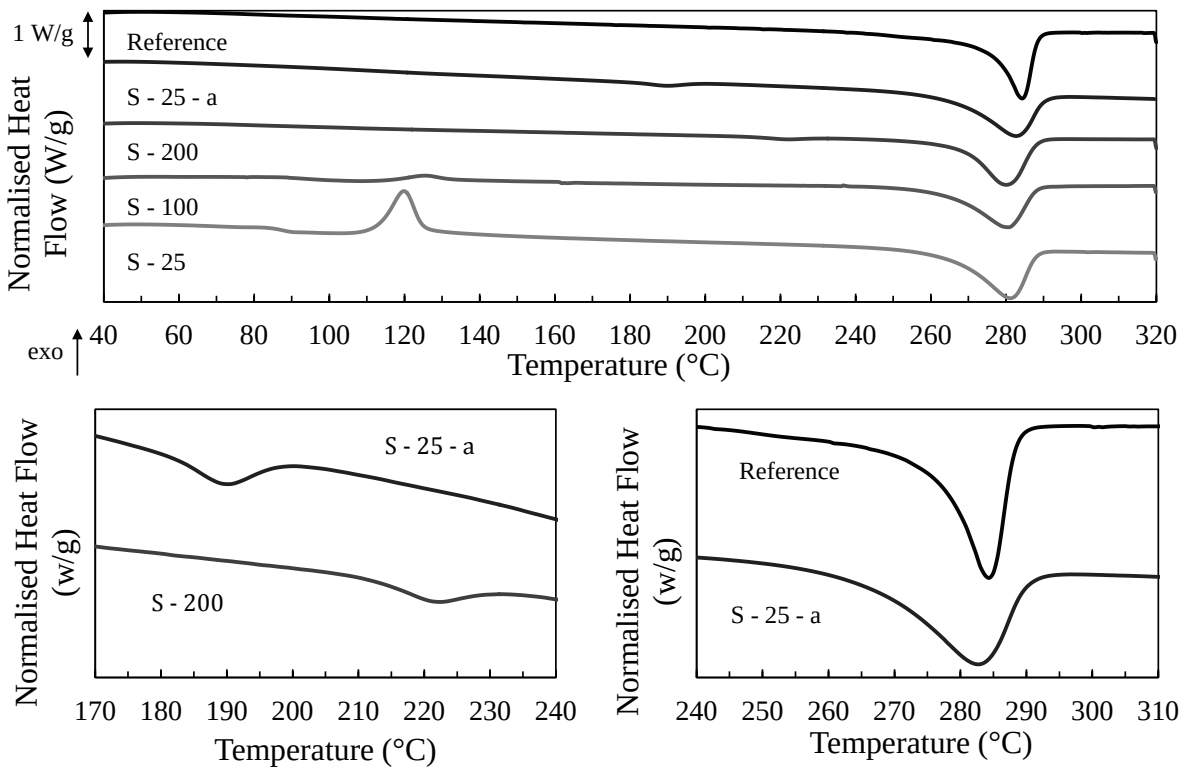

Figure 7: Upper figure) DSC trace for the first heating run of the different samples. From top to bottom: Reference specimen, S-25-a, S-200, S-100, S-25. Bottom left) Close-up look at the secondary fusion peak. Bottom right) Close-up look at the main fusion peak. The curves have been shifted along the vertical axis for clarity.

Table 3.4 shows the average degree of crystallinity with its standard deviation based on the measurements on three specimens per sample. The press-consolidated Reference sample showed the highest degree of crystallinity, followed by the two annealed samples and the S-200 sample. Although the degree of crystallinity increased significantly after annealing, it did not reach the same value as that in the Reference sample. Probably the already existing, less perfect, lamella formed at lower temperature during cooling constrain the development of further crystallinity during the annealing treatment. The stamp-formed samples showed a close relation between the mould temperature and the degree of crystallinity, where the higher mould temperature resulted in a higher degree of crystallinity.

Sample	Degree of crystallinity (%)
Reference	33.3±1.3
S-200	28.1±1.4
S-100	22.4±1.9
S-25	12.1±2.1
S-100-a	27.3±0.8
S-25-a	27.4±0.8

Table 3.4: Degree of crystallinity for the different samples. The reported values correspond to the average and the standard deviation of three specimens per sample.

A final observation can be made from the shape of the melting peak, in particular when comparing the Reference specimen with the stamp-formed specimen. The bottom left graph in Figure 3.7 illustrates that the press-consolidated specimen showed a narrow peak with a peak melting temperature of 285 °C, while the stamped-formed specimens before and after annealing showed a wider melting peak with a somewhat lower peak melting temperature. This can be explained by considering the relation between lamella thickness and the melting temperature. Firstly, a narrow melting peak indicates a narrow distribution of lamella thickness [31]. Secondly, the lamella thickness can be related to the cooling rate, with higher cooling rates resulting in a thinner lamella [30]. The lamella in the press-consolidated Reference specimens were formed from the melt at relatively high temperature. The slow cooling rate means that there is plenty of time to form near-perfect, and relatively thick, lamella with a similar size, resulting in a narrow melting peak in the DSC trace when melted. The lamella present in the stamp-formed specimens, both annealed and not annealed, were formed at high cooling rate or as a result of cold crystallisation. These lamella were formed in a less ideal condition, which results in less perfect crystals with a wider distribution of lamella thicknesses, which is reflected in the wider and lower melting peak.

3.3 Interlaminar fracture toughness

The mode I interlaminar fracture toughness of the different samples was characterised for both crack initiation and crack propagation. A few examples of typical force versus displacement curves are shown in the left graph of Figure 3.8. All specimens showed an initial linear loading behaviour. Nevertheless, the specimens that reached higher forces showed a deviation from the linear behaviour with an increase in the apparent stiffness. This deviation from the linear behaviour was correlated to the low thickness of the specimen which results in large displacements of the bending arms. It should be noted that, even though a large displacement of the bending arms was observed during the tests, the interlaminar fracture toughness is still expected to be properly calculated as during the experiments the moment arm (x) was measured instead of the crack length (a). A stable crack propagation was observed in all specimens. During unloading of the specimens that reached higher forces, some residual displacement was still observed at zero force, which could be caused by the aforementioned fibre bridging or could indicate the occurrence of plastic deformation or damage (besides the delamination) during the test. This second observation indicates a deviation from the linear elastic behaviour of the specimen, possibly resulting in a small error in the calculated fracture toughness values. Nevertheless, as the residual displacement is very small, the results are considered valid for comparison purpose.

The fracture toughness as a function of the crack length (R-curves) is shown in the right graph of Figure 3.8 for a Reference, a S-25, S-100 and a S-25-a specimen. The Reference specimens presented a small increase in the interlaminar fracture toughness along with the crack propagation, which could be due to fibre bridging, which was visually observed to occur in an approximately 10 mm-long area behind the crack tip. Although stable crack propagation was observed for all the stamp-formed specimens, some variability of the fracture toughness along the crack length was observed within each specimen.

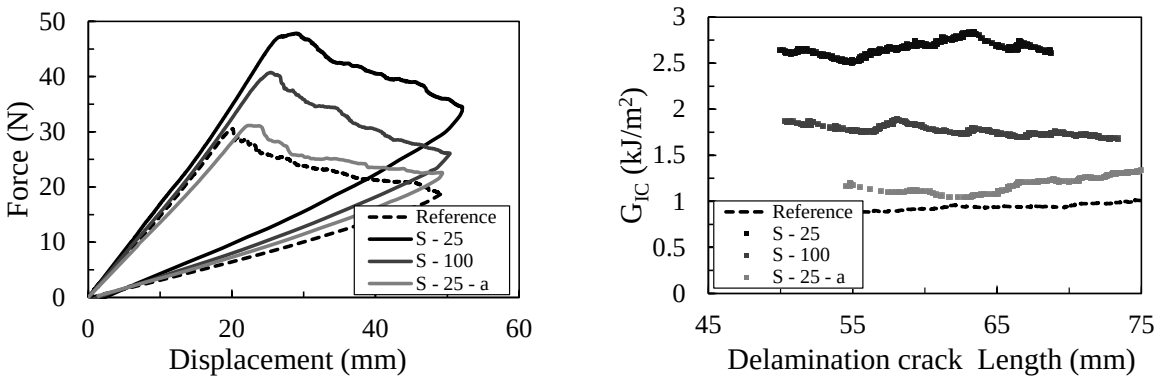

Figure 8: Left) Example of force vs. displacement curves. The difference in the initial compliance among the specimens was attributed to a different initial crack length. Right) An example of R-curves for different specimens. For the name of the specimens the reader is referred to Table 1.

Table 3.5 shows the average initiation and propagation toughness values with their corresponding standard deviation for all the samples. The average initiation value of each sample was calculated by averaging the initiation values of the specimens within that sample. The average propagation value per sample was determined by averaging the mean propagation value of each specimen within that sample. The initiation fracture toughness values were found to be lower than the propagation values. For the Reference specimens, this difference was associated with an increasing R-curve. In the case of the stamp-formed specimens, the effect of a possible increasing R-curve may be hidden behind the higher variability. The S-25 and S-100 samples showed the largest variability in propagation values as can be seen from Table 3.5.

Sample	G_{IC} initiation (kJ/m^2)	G_{IC} propagation (kJ/m^2)	Degree of crystallinity (%)
Reference	0.95±0.10	1.10±0.11	33.3±1.3
S-200	1.11±0.17	1.26±0.19	28.1±1.4
S-100	1.48±0.30	1.68±0.33	22.4±1.9
S-25	2.22±0.41	2.41±0.59	12.1±2.1
S-100-a	1.25±0.18	1.26±0.20	27.3±0.8
S-25-a	1.17±0.19	1.18±0.22	27.4±0.8

Table 3.5: Values measured for interlaminar fracture toughness initiation and propagation.

A small increase of around 10 % in the interlaminar fracture toughness, both in initiation and propagation, was observed when comparing the Reference sample and the S-200 sample.

This reflects that the Processing conditions have an effect in the interlaminar fracture toughness. Moreover, an increase in the interlaminar fracture toughness of more than 100 % between the press sample and the S-25 sample was observed. This shows that the mould temperature has a large effect in the interlaminar fracture toughness.

3.4 Fractographic analysis

The fracture surfaces of the specimens after DCB testing were investigated in order to correlate features of the fracture surface, the interlaminar fracture toughness values and the degree of crystallinity. Figure 3.5 shows the two extreme cases of the fractographic images obtained by scanning electron microscope (SEM). The images correspond to a press-consolidated (Reference) specimen, left figure, and the right figure corresponds to a stamp-formed specimen, with mould temperature of 25 °C (S-25). The images were selected to highlight the most significant differences. It can be observed that the plastic deformation of the matrix in the right figure is higher with respect to the left figure. This is evidenced by increased out of plane drawing of the matrix forming long lips at the edge of the fibres in the S-25 specimen; this fractographic feature is known as “shear lips” in the literature [32]. As expected, the plastic deformation of the matrix increases with decreasing degree of crystallinity.

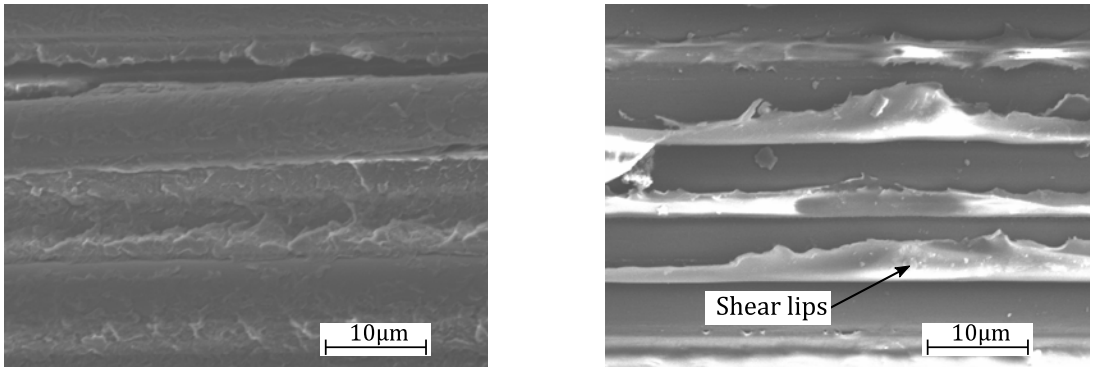

Figure 9: SEM micrographs of two fracture surfaces. Left) Reference specimen. Right) stamp-formed specimen with moulds at 25 °C (S-25) specimens.

Literature reports that the interface adhesion strength between the matrix and the fibres

decreases with a decreasing degree of crystallinity [23]. In the SEM images, it can be seen that for the Reference specimens, the surface of some fibres is covered by matrix, thus some adhesion between fibre and matrix is shown. In the case of the S-25 specimen, however, the fibres show a smooth surface, which suggests that the matrix was separated from the fibres during fracture. Hence apart from showing that crystallinity has an effect on the ductility of the matrix, the results presented in this study show some indications of an effect of the crystallinity on the fibre-matrix interface.

4 Discussion

This section first combines the results from the DSC and DCB experiments to investigate and discuss the interrelation between the degree of crystallinity and fracture toughness. Subsequently, at the end of the section the experimental procedure followed is critically reviewed.

Figure 3.10 shows a plot of the mode I interlaminar fracture toughness (initiation and propagation values) as a function of the degree of crystallinity. The samples with a lower degree of crystallinity show higher scatter in the interlaminar fracture toughness. This high scatter may possibly be attributed to a variation in the degree of crystallinity between the different specimens from the same laminate. This idea is reinforced by the observation that the scatter in the interlaminar fracture toughness is significantly reduced after annealing.

Despite the high scatter in the data on the left side of the graph, a linear correlation can be observed between the interlaminar fracture toughness and the degree of crystallinity, with the interlaminar fracture toughness decreasing with increasing degree of crystallinity. In the most extreme case, an increase of the degree of crystallinity from 12 to 33 % results in a drop of 50% in interlaminar fracture toughness. Arguably more relevant to the industry is the difference between ‘standard’ stamp forming, for which mould temperature around 200 °C is used, and slow press consolidation. The small difference in crystallinity of 28 % vs. 33%

already results in a difference of roughly 10 % in toughness. The aforementioned linear relation between crystallinity and toughness is somewhat surprising as the thermal history not only affected the degree of crystallinity, but also the crystalline morphology, as was evidenced by the variations in melting peaks between the samples. The obtained linear relation may suggest that toughness is mainly influenced by the degree of crystallinity, while the actual morphology has a negligible influence.

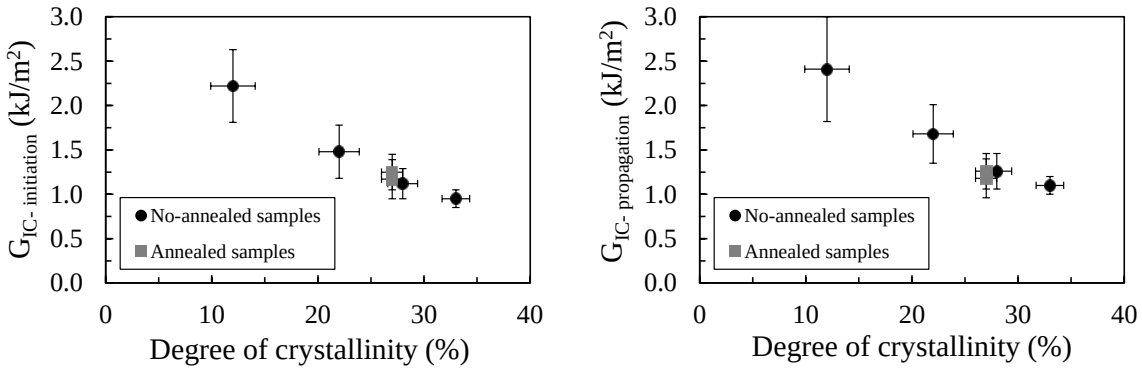

Figure 10: Initiation (left) and propagation (right) interlaminar Fracture toughness vs. degree of crystallinity.

The fractographic analysis showed an increase in the plastic deformation of the matrix with a decrease in the degree of crystallinity of the matrix. Moreover, an indication of a reduction of the matrix fibre bond quality with decreasing degree of crystallinity was observed. The interlaminar fracture toughness was reported to depend on both the ductility of the matrix and on the strength of the fibre-matrix interface [33]. In the range tested, the increase in matrix ductility seems to be the dominant mechanism. The large plastic deformation observed in the fractographic images is localised only at the fracture surface. The global linear elastic behaviour of the specimen during testing was almost not affected by the presence of this plasticity. As such, the tests performed in this research are considered to still comply with the LEFM assumption, which makes the comparison of the values obtained for the different samples acceptable. Lastly, in this study only the interlaminar fracture toughness was evaluated. Nevertheless, from the literature, it is clear that other mechanical properties such

as short beam strength, tensile strength or modulus will decrease with decreasing degree of crystallinity. Given the emergence of new and faster processing techniques, it would be interesting and worthwhile to evaluate the effect of a low degree of crystallinity, even lower than the levels investigated in this work, on other mechanical properties as well.

5 Conclusions

The effect of the degree of crystallinity on the interlaminar fracture toughness of UD Carbon/PPS laminates was investigated experimentally. A stamp forming process was successfully used to obtain well consolidated laminates, i.e. without the presence of voids, at different cooling rates by changing the mould temperature. A maximum average cooling rate of 3500 °C/min was achieved for a mould temperature of 25 °C. The crystallinity and interlaminar toughness were characterised using DSC and DCB tests, respectively.

Laminates stamp formed with a mould temperature of 200 °C, which is typical industrial procedure for this material system, had a high degree of crystallinity (28 %) but not as high as that in the reference press-consolidated sample (33 %). The small decrease in the degree of crystallinity from 33 % to 28 % was observed to result in roughly a 10 % increase in the interlaminar fracture toughness. A lower degree of crystallinity was obtained for lower mould temperatures. For the extreme case of a mould temperature of 25 °C, a degree of crystallinity as low as 12 % was obtained. The interlaminar fracture toughness was observed to increase more than 100 % with a change in degree of crystallinity from 33 % to 12 %. Microscopy on the fracture surfaces showed that the main mechanism increasing the interlaminar fracture toughness was the larger local plastic deformation that the PPS can undergo with lower degree of crystallinity.

Clearly, the effect of the degree of crystallinity on the mechanical performance, and more particularly the toughness, has to be taken into account when designing components to be manufactured with processing technologies which have fast cooling rates. This is especially

true for relatively new processes such as ultrasonic welding or AFP, for which even higher cooling rates are observed than those studied in this work.

6 Acknowledgements

The authors gratefully acknowledge the financial as well as technical support from the industrial and academic members of the ThermoPlastic composites Research Center (TPRC) as well as the support funding from the Province of Overijssel for improving the regional knowledge position within the Technology Base Twente initiative.

7 References

[1] A. Kelly, “Concise encyclopedia of composite materials,” Elsevier, 2012.

[2] R. C. Harper, “Thermoforming of thermoplastic matrix composites. Part II,” SAMPE J., vol. 28, no 2, 1992.

[3] E. Wang and T. Gutowski, “Cost comparison between thermoplastic and thermoset composites,” SAMPE J, vol. 26, pp. 19-26, 1990.

[4] T. G. P. Gutowski, “Advanced Composites Manufacturing,” John Wiley & Sons, 1997.

[5] A. Offringa, “New thermoplastic composite design concepts and their automated manufacture,” JEC Compos Mag, vol. 58, pp. 45-49, 2010.

[6] A. Offringa, “Thermoplastic composites—rapid processing applications,” Composites Part A: Applied Science and Manufacturing, vol. 27, no 4, pp. 329-336, 1996.

[7] J. J. Tierney and J. W. Gillespie Jr., “Crystallization kinetics behavior of PEEK based composites exposed to high heating and cooling rates,” Composites Part A: Applied Science and Manufacturing, vol. 35 , no 5, pp. 547-558, 2004.

[8] W. J. B. Grouve, L. L. Warnet, B. Rietman, H. A. Visser, and R. Akkerman, “Optimization of the tape placement process parameters for Carbon–PPS composites,” Composites Part A: Applied Science and Manufacturing, vol. 50, pp. 44-53, 2013.

[9] P. Davies, M. L. Benzeggagh and F. X. De Charentenay, “Delamination behavior of Carbon-fiber-reinforced PPS,” SAMPE Q., (United States), vol. 19, no 1, 1987.

[10] D. Traudel-broucher, A. L. Esquirol and M. N. Bureau, “Influence of cooling rates on microstructure and mechanical performance of continuous fiber reinforced PPS composites,” SAMPE International Symposium and Exhibition-Emerging Opportunities, 2012.

[11] N. L. Batista, P. Olivier, G. Bernhart, M. C. Rezende, and E. C. Botelho, “Correlation between degree of crystallinity, morphology and mechanical properties of PPS/Carbon fiber laminates,” Materials Research, vol. 19, no 1, pp. 195-201, 2016.

[12] J. Deporter and D. G. Baird, “The effects of thermal history on the structure/property relationship in polyphenylene-sulfide/Carbon fiber composites,” Polymer Composites, vol. 14, no 3, pp. 201-213, 1993.

[13] J. E. Spruiell, “A review of the measurement and development of crystallinity and its relation to properties in neat poly (phenylene sulfide) and its fiber reinforced composites,” No. ORNL/TM-2004/304. ORNL, 2005.

[14] P. T. Curtis, P. Davies, I. K. Partridge and J. P. Sainty, “Cooling rate effects in PEEK and Carbon fibre-PEEK composites,” Elsevier Proceedings of the sixth international conference on composite materials (ICCM 6/ECCM 2), vol. 4, pp. 401-412, 1987.

[15] M. F. Talbott, G. S. Springer and L. A. Berglund, “The effects of crystallinity on the mechanical properties of PEEK polymer and graphite fibre reinforced PEEK,” Journal Compos Mater, vol. 21, no 11, pp. 1056-

1081, 1987.

[16] G. M. Ostberg and J. C. Seferis, “Annealing effects on the crystallinity of polyetheretherketone (PEEK) and its Carbon fibre composite,” Journal Appl Polym Sci, vol. 33, no 1, pp. 29-39, 1987.

[17] P. Davies, W. J. Cantwell, C. Moulin and H. H. Kausch, “A study of the delamination resistance of IM6/PEEK composites,” Composites Science and Technology, vol. 36, no 2, pp. 153-166, 1989.

[18] A. Lustiger, F. S. Uralil and G. M. Newaz, “Processing and structural optimisation of PEEK composites,” Polym Compos, vol. 11, no 1, pp. 65-75, 1990.

[19] P. Vautey, “Cooling rate effects on the mechanical properties of a semicrystalline thermoplastic composite,” SAMPE Q; vol. 21, no 2, pp. 23-28, 1990.

[20] P. Davies, W. J. Cantwell, P. Y. Jar, H. Richard, D. J. Neville and H. H. Kausch, “Cooling rate effects in Carbon fibre/PEEK composites,” ASTM STP - Composite Materials: Fatigue and Fracture, vol. 3, pp. 70-80, 1991. DOI: 10.1520/STP17713S

[21] J. Denault and T. Vu-Khanh, “Crystallisation and fibre/matrix interaction during the molding of PEEK/Carbon composites,” Polymer composites, vol. 13, no 5, pp. 361-371, 1992.

[22] T. Vu-Khanh and J. Denault, “Effect of molding parameters on the interfacial strength in PEEK/Carbon composites,” Journal of reinforced plastics and composites, vol. 12, no 8, pp. 916-931, 1993.

[23] S. L. Gao and J. K. Kim, “Cooling rate influences in Carbon fibre/PEEK composites. Part II: interlaminar fracture toughness,” Composites Part A: Applied science and manufacturing, vol. 32, no 6, pp. 763-774, 2001.

[24] A. Beehag, and L. Ye, “Influence of cooling rate on interlaminar fracture properties of unidirectional commingled CF/PEEK composites,” Applied Composite Materials, vol. 2, no 3, pp. 135-151, 1995.

[25] S. L. Gao and J. K. Kim, “Correlation among crystalline morphology of PEEK, interface bond strength, and in-plane mechanical properties of Carbon/PEEK composites,” Journal of applied polymer science, vol. 84, no 6, pp. 1155-1167, 2002.

[26] L. C. López and L. W. Garth, “Crystallization kinetics of poly (p-phenylene sulphide): effect of molecular weight,” Polymer, vol. 29, no 1, pp. 106-113, 1988.

[27] W. I. Lee and G. S. Springer, “A model of the manufacturing process of thermoplastic matrix composites,” Journal of composite materials, vol. 21, no 11, pp. 1017-1055, 1987.

[28] J. G. Williams, “Large displacement and end block effects in the 'DCB' interlaminar test in modes I and II,” Journal of Composite Materials, vol. 21, no 4, pp. 330-347, 1987.

[29] M. Bonnet, K. D. Rogausch and J. Petermann, “The endothermic “annealing peak” of poly (phenylene sulphide) and poly (ethylene terephthalate),” Colloid and Polymer Science, 1999, vol. 277, no 6, pp. 513-518, 1999.

[30] P. Cebe and S. Chung, “Melting behavior of high performance composite matrix polymers: Poly (phenylene sulfide),” Polymer Composites, vol. 11, no 5, pp. 265-273, 1990.

[31] J. I. Lauritzen Jr and J. D. Hoffman, “Extension of theory of growth of chain-folded polymer crystals to large undercoolings,” Journal of applied Physics, vol. 44, no 10, pp. 4340-4352, 1973.

[32] D. Purslow, “Matrix fractography of fibre-reinforced thermoplastics, Part 1. Peel failures,” Composites, vol. 18, no 5, pp. 365-374, 1987.

[33] L. Drzal and M. Madhukar, “Fibre-matrix adhesion and its effect on composite mechanical properties,” Journal of materials science, vol. 28, no 3, pp. 569-610, 1991.

1